Regulation of T cell activation, anxiety, and male aggression by RGS2

Antonio J. Oliveira-dos-Santos*, Goichi Matsumoto*, Bryan E. Snow*, Donglin Bai†, Frank P. Houston‡, Ian Q. Whishaw§, Sanjeev Mariathasan¶, Takehiko Sasaki*, Andrew Wakeham*, Pamela S. Ohashi¶, John C. Roder†, Carol A. Barnes‡, David P. Siderovski‖, and Josef M. Penninger*,**

*Amgen Institute and ¶Ontario Cancer Institute, Departments of Medical Biophysics and Immunology, University of Toronto, 620 University Avenue, Toronto, ON M5G 2C1 Canada; †Samuel Lunenfeld Research Institute, Mount Sinai Hospital, Toronto, ON M5S1A8 Canada; ‡Arizona Research Laboratories, Division of Neural Systems, Memory, and Aging, University of Arizona, Tucson, AZ 85724; §Department of Psychology, University of Lethbridge, AB T1K3 M4 Canada; and ‖Department of Pharmacology, University of North Carolina, Chapel Hill, NC 27599

Communicated by Alfred G. Gilman, University of Texas Southwestern Medical Center, Dallas, TX, August 29, 2000 (received for review June 20, 2000)

Regulators of G protein signaling (RGS) proteins accelerate the GTPase activity of Gα protein subunits *in vitro*, negatively regulating G protein-coupled receptor signaling. The physiological role of mammalian RGS proteins is largely unknown. The RGS family member *rgs2* was cloned as an immediate early response gene up-regulated in T lymphocytes after activation. To investigate the role of RGS2 *in vivo*, we generated *rgs2*-deficient mice. We show that targeted mutation of *rgs2* in mice leads to reduced T cell proliferation and IL-2 production, which translates in an impaired antiviral immunity *in vivo*. Interestingly, *rgs2*$^{-/-}$ mice also display increased anxiety responses and decreased male aggression in the absence of cognitive or motor deficits. RGS2 also controls synaptic development and basal electrical activity in hippocampal CA1 neurons. Thus, RGS2 plays an important role in T cell activation, synapse development in the hippocampus, and emotive behaviors.

G protein-coupled receptors (GPCR) control fundamental cellular processes ranging from embryogenesis and neurotransmitter release to cell survival, proliferation, and differentiation. Heterotrimeric G proteins are composed of α, β, and γ subunits that relay GPCR stimulation to downstream signaling pathways (1). On ligand binding, GPCR undergoes conformation changes of its intracellular loops that promote the exchange of GDP for GTP on Gα and the subsequent dissociation of Gα and G$\beta\gamma$. Both GTP-bound Gα and free G$\beta\gamma$ propagate the signal through interactions with downstream effectors. Deactivation of GPCR signaling depends on the rate of Gα GTP hydrolysis.

Studies of GPCR desensitization have led to the discovery of a large and evolutionarily conserved family of GTP-activating (GAP) factors for Gα termed "regulators of G protein signaling" (RGS). RGS proteins share an RGS domain ($\approx$120 amino acids) capable of accelerating Gα-dependent GTP hydrolysis and the conversion of active GTP-bound Gα to its inactive GDP-bound form (2–7). The first RGS identified was the yeast protein Sst2, isolated in a screen for mutants that failed to down-regulate the GPCR-mediated response to mating pheromone (8–9). Over 20 mammalian RGS proteins have been identified (7, 10). Recently it has been shown that RGS9–1 controls the photosensitization response in the mouse eye (11). Axin, which contains a RGS domain, negatively regulates the Wnt-signaling pathway, and *axin*-mutant mice display defects in embryonic axis formation (12). However, Axin has no detectable GAP activity for Gα (10). The physiological roles of other mammalian RGS proteins are yet to be established.

The RGS family member *rgs2* was cloned as an early response gene up-regulated in activated T cells (13–14). RGS2 is also up-regulated in central nervous system (CNS) neurons after stimuli that evoke long-term neuronal plasticity (15–16). *In vitro*, RGS2 interacts with G$\alpha_{q/11}$ and stimulates its GTPase activity (17–18), and RGS2 overexpression in cells inhibits Gα_i- (15) and Gα_s-dependent (19) signaling. To investigate the role of RGS2 *in vivo*, we generated *rgs2*-deficient mice. *rgs2* deficiency in mice leads to impaired T cell activation *in vitro* and *in vivo*. Interestingly, mice lacking RGS2 also exhibit reduced male aggressive behavior and increased anxiety, whereas morphological and electrophysiological analyses indicate a role for RGS2 in hippocampal CA1 neuron function.

Materials and Methods

***rgs2* Mutant Mice.** RGS2 exons 4 and 5 encoding the RGS domain were replaced with PGK-Neo^R in antisense orientation. G418-resistant E14K embryonic stem (ES) cells were screened by PCR and Southern blot for homologous recombination. Targeted ES cell clones were injected into C57BL/6 blastocysts and heterozygous *rgs-2*$^{+/-}$ mice obtained by mating chimeras with C57BL/6J mice. PCR primers: wild-type allele (5′-CCGAGTTCTGTGAAGAAAACATTG3′; 5′GGGACTCCTGGTCTCATGTAGCAT3′) and mutant allele (5′-GCTAAAGCGCATGCTCCAGAC-3′; 5′-GGCCCA-CATTTACACGAACC-3′). All experiments were carried out by using littermate mice on a C57BL/6J background (F5 generation), and mice were maintained in accordance with institutional guidelines.

Immunocytometry. Single-cell suspensions of thymi, lymph nodes, and spleens were stained with FITC-, phycoerythrin-, or biotin-conjugated Abs reactive to CD3ε, TCR$\alpha\beta$, CD4, CD8, CD25, CD44, CD28, CD69, CD11b (Mac-1), CD11c, B220, CD43, sIgM, sIgD, or Gr-1. Biotinylated antibodies were visualized by using streptavidin-RED670. Samples were analyzed by flow cytometry by using a FACScan (Becton Dickinson).

T and B Cell Assays. For proliferation assays, freshly isolated T cells were activated with PMA (10 ng/ml, phorbol myristate acetate) plus Ca^{+2} ionophore (100 ng/ml, ionomycin), soluble anti-CD3ε (0.1–1 μg/ml, clone 145–2C11), anti-CD28 (0.02–0.2 μg/ml, clone 37.51), or recombinant mouse IL-2 (50 units/ml) in triplicate for 12, 24, 48, 72, or 120 h, followed by a 12-h pulse with [^{3}H]thymidine (1 μ Ci/ml). Cytokine production was determined by ELISA. For B cell analysis, splenic B lymphocytes were purified (90–95% B220$^+$ cells) by negative magnetic sorting and activated with various stimuli. Basal serum Ig levels (IgM, IgG1, IgG2a, IgG2b, IgG3, and IgA) were determined by ELISA (20). For lymphocytic choriomeningitis virus (LCMV) infections,

Abbreviations: GPCR, G protein-coupled receptors; GAP, GTP-activating; RGS, regulators of G protein signaling; CNS, central nervous system; ES, embryonic stem; LCMV, lymphocytic choriomeningitis virus; EPSP, excitatory postsynaptic potentials.

**To whom reprint requests should be addressed. E-mail: jpenning@amgen.com.

The publication costs of this article were defrayed in part by page charge payment. This article must therefore be hereby marked "*advertisement*" in accordance with 18 U.S.C. §1734 solely to indicate this fact.

Article published online before print: *Proc. Natl. Acad. Sci. USA*, 10.1073/pnas.220414397. Article and publication date are at www.pnas.org/cgi/doi/10.1073/pnas.220414397

mice were infected with LCMV (700 plaque-forming units, s.c.) into the hind footpad. Cellular infiltration was measured daily as described (21).

Behavior Studies. Four- to five-month-old sex-matched littermate mice were examined for neuromotor functions (22): vibrissae, eyes, rearing/support/standing, muscle tone, tail hanging-induced turns and limbs/digits extension, ear reflex, eye blink and pupillary response to light, sweet/bitter tasting acceptance/rejection, and orientation toward sound. Circadian and open-field activities (i.e., cage crosses, total distance, vertical movements) were measured in cages fitted with infrared sensors. Exploration test was performed by putting the mice in the center of a white disk (183-cm diameter), with or without objects distributed in four quadrants. The mice were video tracked (seven trials). Fecal pellets and rears were counted. Motor coordination was analyzed by a rotating rod task. For a balance task, a mouse was held by the tail and allowed to grasp a suspended horizontal wooden rod (3 mm Ø) with its hind limbs, with recording of the time for the mouse to pull itself into balance and the number of falls.

Mice were studied in a spatial water maze for 7 days with a hidden platform in the southwest quadrant (22). On day 7, a final probe trial (60 s in the pool without platform) was applied. From day 8 to 16, tests were reassumed with the platform moved to the northeast quadrant (reversal, 2 trials per day). Time to find the platform and total distance were measured. In the T-maze test, on day 1 the mice were placed in an empty maze for 10 min with access only to its central and right arms. Several objects were placed as cues around the maze. On day 2, each subject was again placed in the T-maze and given access to the left arm of the maze. The mice were observed for 5 min, with recording of time spent in the new area and first choice. Step-down avoidance test was also carried out, in which the mice were required to remember that prior stepping off a safe platform resulted in a foot shock (1 s, 0.12 mA). Latency on the platform was recorded in each trial. Aggression was tested by using displacement from a plastic tube (30 cm long and 3.05 cm Ø). A *rgs2*$^{-/-}$ and littermate control mouse were released into either end of the tube, with the first mouse to exit being deemed the "loser," that is, this mouse was deemed to be the less aggressive of the two. For light/dark preference tests, cages were divided into dark and light halves and the time spent by each mouse in each half measured.

Electrophysiology. Electophysiology studies were carried out as described (23). Single hippocampal slices (400 μm) were superfused with artificial cerebrospinal fluid (2 ml/min; saturated with 95% O_2 and 5% CO_2 at 30°C). Field potentials were sampled at 10 kHz and analyzed with PCLAMP6 software (Axon Instruments, Foster City, CA). Field excitatory postsynaptic potentials (EPSP) were recorded with a micropipette (2–4 MΩ) placed in the stratum radiatum of CA1 area. Stimulation was delivered at Schaffer collateral. Test stimulus frequency was 0.1 Hz. The tetanic stimulation consisted of four trains of 100-Hz stimulation lasting 500 ms at 10-s intervals. EPSP slope was calculated from linear regression of the rising phase 10–65% of the peak response. The baseline value of EPSP slope was that from the first 5-min period and was defined as 100%. Input/output relationship was constructed by plotting the amplitude of presynaptic volley (input) vs. EPSP slope (output).

Results and Discussion

***rgs2* Gene Targeting.** The *rgs2* locus was inactivated in ES cells by replacing exons 4 and 5 corresponding to the RGS domain (Fig. 1*A*). Chimeric mice were bred to obtain germ-line transmission

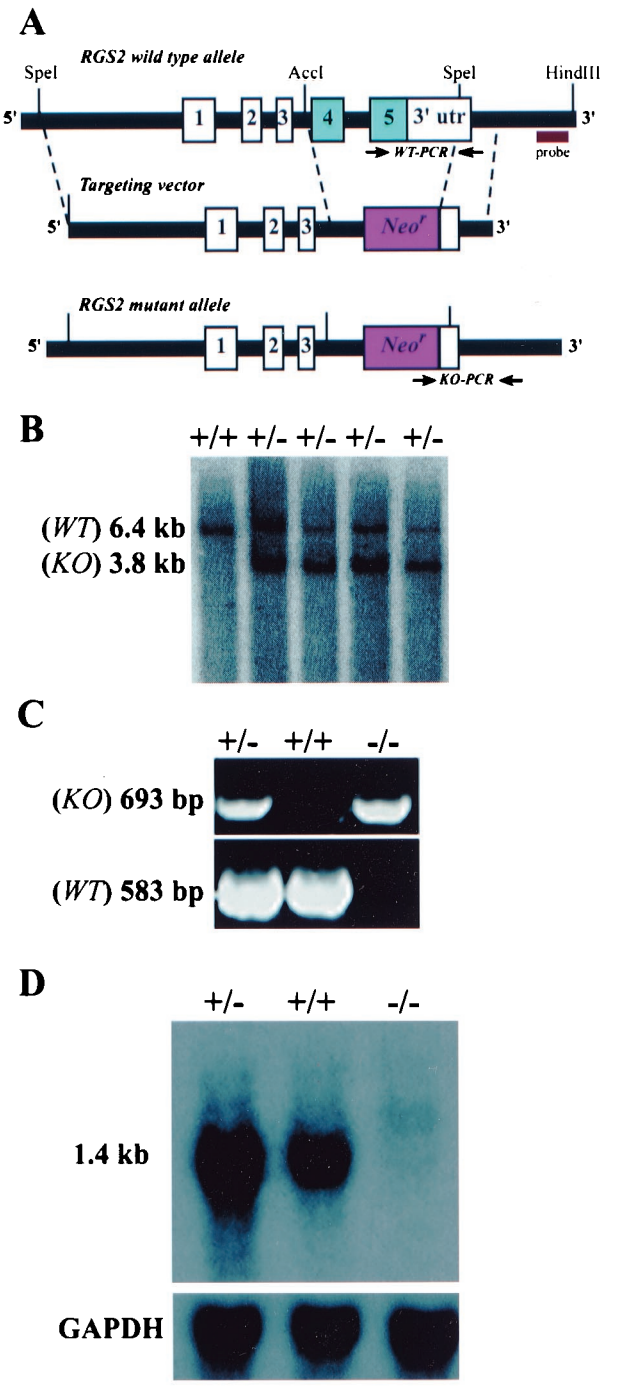

Fig. 1. Generation of *rgs2*-deficient mice. (*A*) *rgs2* targeting vector. (*B*) Southern blot (see 3′ flanking probe in *A*) from *rgs2* mutant ES cell clones. Wild-type (*WT*) and mutant (*KO*) bands are shown. (*C*) Genotyping of *rgs2* mice. WT and KO PCR primers are shown in *A* (arrows). Loss of the wild-type *rgs2* allele was confirmed by genomic Southern blot. (*D*) Northern blot analysis of brain mRNA from *rgs2* WT (+/+), heterozygous (+/−), and KO (−/−) mice (full-length *rgs2* cDNA probe).

of the mutated *rgs2* allele (Fig. 1 *B* and *C*). The *rgs2* mutation proved to be null, as shown by Northern blot analyses of brain tissue (Fig. 1*D*). *rgs2*$^{-/-}$ mice were born at the expected Mendelian frequency, were fertile, and displayed normal growth. No anatomical or histological abnormalities were observed. Differentiation of all hematopoietic lineages, including neutrophils, macrophages, erythrocytes, and platelets, was normal in *rgs2*$^{-/-}$ mice.

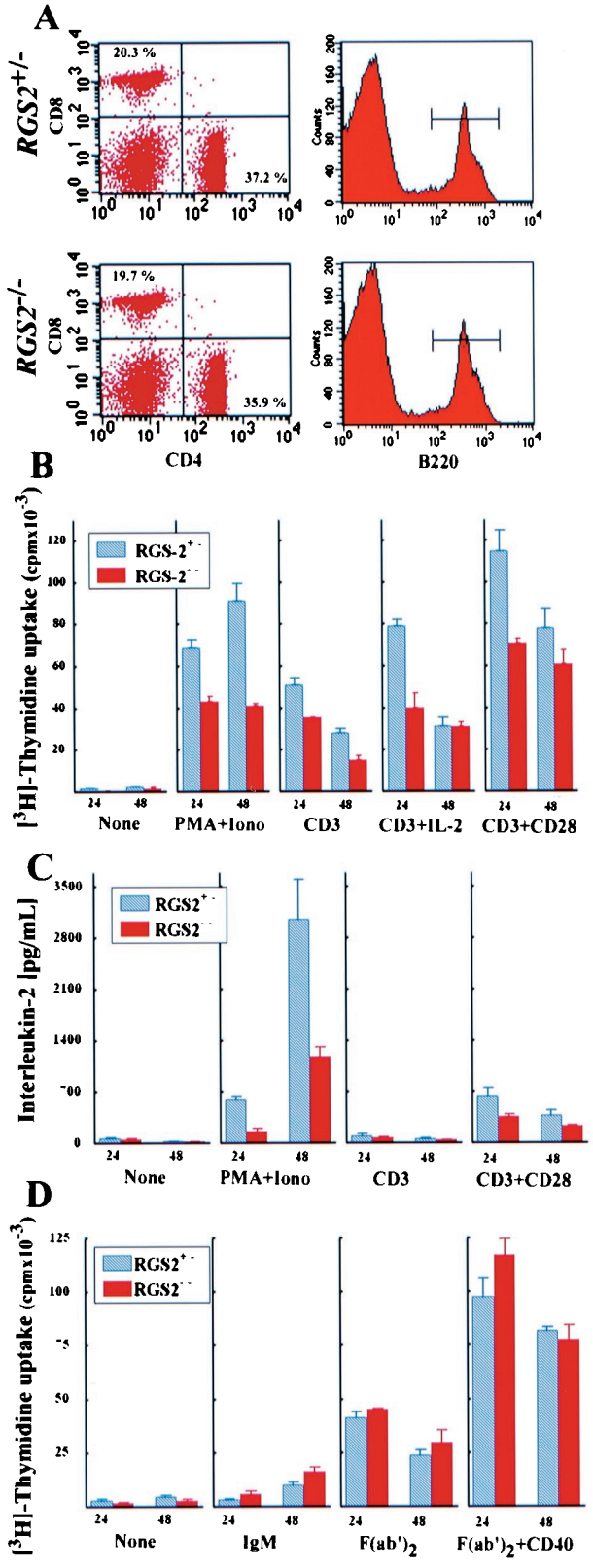

Fig. 2. Impaired proliferation and IL-2 production by *rgs2*$^{-/-}$ T cells. (*A*) Normal populations of CD4$^+$ and CD8$^+$ T cells and B220$^+$ B cells in lymph nodes of *rgs2*$^{-/-}$ mice. Numbers in each quadrant represent percentages of each subset. (*B*) Proliferation. Lymph node T cells (2×10^5/well) from *rgs2*$^{-/-}$ and *rgs2*$^{+/-}$ mice were activated by using PMA [10 ng/ml]+Ca^{+2}-ionophore [100 ng/ml], TCR stimulation [anti-CD3α mAb (0.1 μg/ml)] with and without CD28 costimulation [anti-CD28 mAb (0.02 μg/ml)] or IL-2 [50 units/ml]. Results are shown as mean [^{3}H]thymidine uptake ± SD. Difference in proliferation between *rgs2*$^{+/-}$ and *rgs2*$^{-/-}$ T cells was statistically significant (*t* test, $P < 0.05$). (*C*) IL-2 production. Lymph node T cells were activated as above, and IL-2 was measured by ELISA at 24 and 48 h poststimulation. Mean values of IL-2 production ± SD are shown. (*D*) Activation of B cells. Purified splenic B cells (1×10^5/well) were incubated in triplicate for 24 and 48 h in medium alone (None) or medium containing anti-IgM (20 μg/ml), anti-IgM (Fab')$_2$ (15 μg/ml) with or without anti-CD40 (5 μg/ml). Results are shown as mean [^{3}H]thymidine uptake ± SD.

Defective Proliferation and IL-2 Production by *rgs2*$^{-/-}$ T Cells. Because RGS2 expression is induced in activated T cells after TCR engagement or stimulation by mitogens such as ConA or PMA plus Ca^{2+} ionophore (PMA + Iono) (ref. 14 and data not shown), we determined whether RGS2 plays a role in T cell activation. *rgs2*$^{-/-}$ mice displayed normal numbers and subsets of CD4$^+$ and CD8$^+$ T cells and B cells in lymphoid organs (Fig. 2*A*). The surface levels of TCR$\alpha\beta$, CD3, CD4, CD8, CD28, CD45, CD5, H2K^b, CD44, LFA1, CD25, and CD69 on both splenic and lymph node peripheral CD4$^+$ and CD8$^+$ T cells were comparable in *rgs2*$^{+/-}$ and *rgs2*$^{-/-}$ mice (not shown). To examine peripheral T cell function, T cells from the lymph nodes of *rgs2*$^{+/-}$ and *rgs2*$^{-/-}$ littermates were stimulated with anti-CD3ε mAb, anti-CD3ε plus anti-CD28 mAbs, or PMA plus Ca^{2+}-ionophore. The proliferation *in vitro* of *rgs2*$^{-/-}$ T cells was significantly reduced in response to TCR engagement, a deficit that could not be overcome by CD28 costimulation (Fig. 2*B*). Consistent with the identification of RGS2 as an early response gene in activated T cells (13–14), the proliferative defect was most obvious at 24 h of stimulation. Induction and kinetics of apoptosis were comparable among *rgs2*$^{+/-}$ and *rgs2*$^{-/-}$ T cells (not shown). Thus, RGS2 acts as an immediate early gene downstream of TCR activation in T cells.

In addition to their proliferative defect, *rgs2*$^{-/-}$ T cells produced significantly lower levels of the T cell growth factor IL-2 compared with controls (Fig. 2*C*). IL-2 insufficiency *per se* does not explain the proliferative deficit because IL-2 supplementation did not restore proliferation to normal (Fig. 2*B*). The high-affinity IL-2 receptor α chain (CD25) and the activation markers CD69, CD44, ICAM1, and CTLA4 were up-regulated to a normal extent and with normal kinetics in *rgs2*$^{-/-}$ T cells in response to TCR engagement or mitogen treatment (not shown). The functional defect in T cell proliferation (Fig. 2*B*) and cytokine production (Fig. 2*C*) can also be observed in *rgs2*$^{-/-}$ T cells treated with PMA/Ca^{2+} ionophore, a stimulus that bypasses the proximal TCR signal. Consistent with this finding, the kinetics and extent of early TCR-mediated signaling events, including Ca^{2+} mobilization, overall tyrosyl phosphorylation, and activation of MAPK and SAPK/JNKs, were normal in *rgs2*$^{-/-}$ lymph node T cells (not shown), suggesting that their proximal TCR signaling pathways are intact.

With regards to B cells, *rgs2*$^{-/-}$ mice displayed normal numbers and differentiation (not shown). *In vitro* proliferation of *rgs2*$^{-/-}$ B cells in response to treatment with anti-IgM Ab, the F(ab′)$_2$ fragment of the anti-IgM Ab, anti-CD40, or LPS was similar to that of *rgs2*$^{+/-}$ B cells (Fig. 2*D* and data not shown). Furthermore, baseline serum Ig levels were equivalent in *rgs2*$^{-/-}$ and *rgs2*$^{+/-}$ mice. Thus, RGS2 is not required for B cell activation. Our results show that antigen receptor-triggered RGS2 expression in T cells is required for proliferation and IL-2 production.

Chemokines are critical regulators of T cell function, signaling via GPCRs expressed on the surface of resting and activated T cells (24). It has also been shown that overexpression of RGS-family members in cell lines can modulate chemokine receptor signaling (18). However, no differences were observed between both resting and preactivated (6-h activation with anti-CD3ε

before chemokine treatment) $rgs2^{+/-}$ and $rgs2^{-/-}$ $CD4^+$ or $CD8^+$ T cells in either proliferation or cell migration in response to the chemokines SDF-1α, RANTES, or MIP-1α (not shown). These results do not preclude regulation by RGS2 of T cell responsiveness to signals mediated by other chemokine receptors. Furthermore, $rgs2^{+/-}$ and $rgs2^{-/-}$ T lymphocytes showed comparable responses to the GPCR agonists lysophosphatidic acid, histamine, and adenosine (not shown). The GPCRs whose functions are under RGS2 control in T cells remain to be identified.

Impaired Immunity in *rgs2*$^{-/-}$ Mice. To determine whether RGS2 plays a role in T cell responses *in vivo*, $rgs2^{+/-}$ and $rgs2^{-/-}$ mice were injected in the footpad with LCMV (21). $rgs2^{+/-}$ mice developed an effective LCMV-induced footpad swelling reaction starting from day 6 postinfection (Fig. 3). In contrast, the footpad swelling reaction was significantly decreased and delayed in $rgs2^{-/-}$ mice, indicating that RGS2 expression is required for an efficient antiviral response *in vivo*. Thus, the *in vitro* deficit in proliferation and IL-2 production by $rgs2^{-/-}$ T cells translates into an impaired anti-virus response *in vivo*, indicating that RGS2 expression is physiologically relevant for normal T cell function. These results provide the first genetic evidence that RGS proteins play a role in the activation of lymphocyte.

RGS2 Controls Male Aggression and Anxiety. During our evaluation of the mutant mice, we noted unusual fighting between male $rgs2^{+/-}$ and $rgs2^{-/-}$ littermates that sometimes resulted in severe injuries. Stimuli triggering long-term plasticity in the CNS induce the up-regulation of RGS2 in the hippocampus, cortex, caudate putamen, striatum, and amygdala (15–16). Because these regions regulate a variety of behavioral pathways, we investigated whether RGS2 plays a role in CNS function. We first determined whether RGS2 deficiency in mice leads to alterations in motor functions. Both $rgs2^{-/-}$ and $rgs2^{+/-}$ littermate mice showed normal motor responses (tests listed in *Materials and Methods*). Circadian activity was normal in the mutant mice (Fig. 4*A*), as was exploratory behavior during two independent open field and exploration tests (not shown). $rgs2^{-/-}$ mice also exhibited appropriate performances in rotating rod (Fig. 4*B*) and balance tests (not shown), confirming the integrity of the neurological pathways responsible for motor coordination and balance. Spatial and conditional learning, as determined by the hidden platform, water maze, and passive avoidance tests, were comparable between $rgs2^{-/-}$ and $rgs2^{+/-}$ littermates. Long-term potentiation in the Schaffer collateral CA1 pathway of individual hippocampus slices was also equivalent in $rgs2^{-/-}$ and $rgs2^{+/-}$

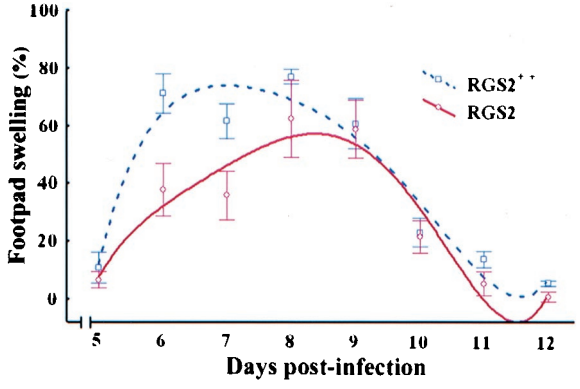

Fig. 3. Reduced LCMV-induced footpad swelling in $rgs2^{-/-}$ mice. Mice were infected in the footpad with LCMV and swelling measured. Average footpad swelling (percentage increase compared with footpads thickness before infection) of six animals per group.

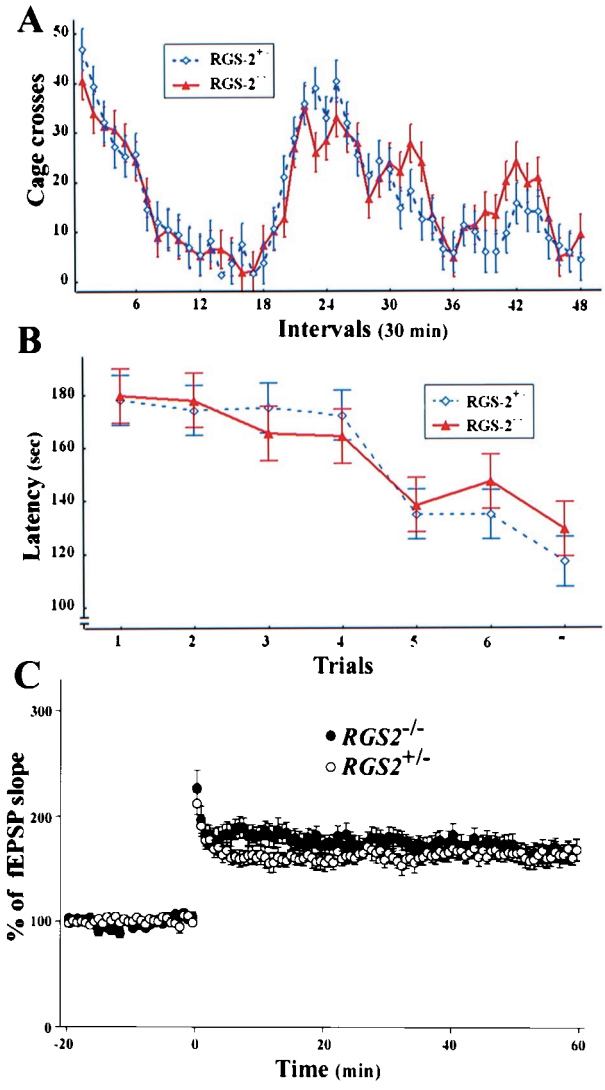

Fig. 4. Normal circadian activity, motor functions, and long-term potentiation (LTP) in $rgs2^{-/-}$ mice. (*A*) Circadian activity was monitored during a 24-h period (12-h light/dark cycles). Mean crosses accumulated per 30-min intervals ± SD are shown. (*B*) Normal motor function in a rotarod test. Mean values of retention times (latency) ± SD are shown. Trials indicate a stepwise increase in rotarod speed (10–40 rpm, 5-rpm increase per trial). (*C*) Tetanus-induced LTP in CA1 neurons. Averaged normalized field EPSP (fEPSP) slope measurements obtained from 11 hippocampus slices of 4 $rgs2^{+/-}$ and 4 $rgs2^{-/-}$ mice.

mice (Fig. 4*C*). These data show that RGS2 deficiency has no apparent effect on motor responses, circadian activity, exploratory behavior, motor coordination, or spatial learning and memory.

Social dominance and territorial aggression are well-characterized behaviors in male mice (25). Intriguingly, $rgs2^{-/-}$ male mice exhibited significantly reduced aggressive behavior compared with their $rgs2^{+/-}$ littermates, whereas the aggressive behavior of $rgs2^{-/-}$ female mice was normal (Fig. 5*A*). Because aggression correlates with anxiety (25), we subjected $rgs2^{-/-}$ male mice to the light/dark preference test. $rgs2^{-/-}$ mice showed a greater preference for the dark compared with $rgs2^{+/-}$ control littermates (Fig. 5*B*), indicating increased anxiety. Consistent with this behavioral phenotype, $rgs2^{-/-}$ mice were found to drop significantly more fecal pellets than $rgs2^{+/-}$ littermates during the light/dark preference test (2.3 ± 0.6 vs. 0.8 ± 0.3 pellets) and

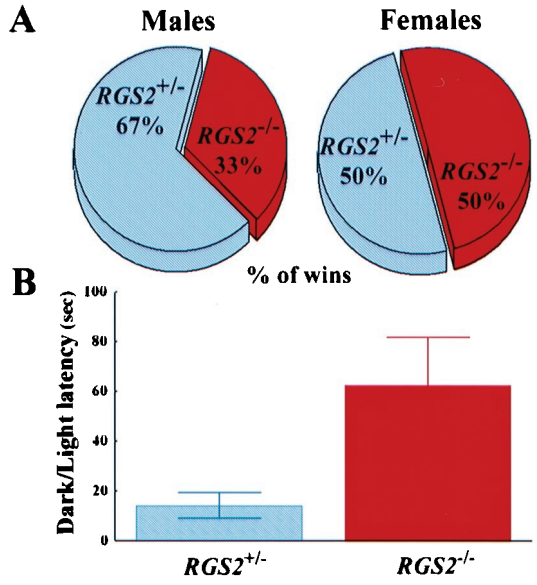

Fig. 5. RGS2 regulates male aggression and anxiety. (*A*) Reduced male aggressive behavior. Aggression was measured in paired groups of male or female *rgs2*$^{-/-}$ and *rgs2*$^{+/-}$ mice by using a replacement test. Results represented as percentages of displacement per group (''wins''). Eighteen trials were carried out for each group. (*B*) Increased anxiety. The anxiety response was measured by using a dark/light preference test. Note the increased preference for the dark environment in *rgs2*$^{-/-}$ mice. The difference in mean dark/light latency ± SD was statistically significant (*t* test; $P < 0.05$).

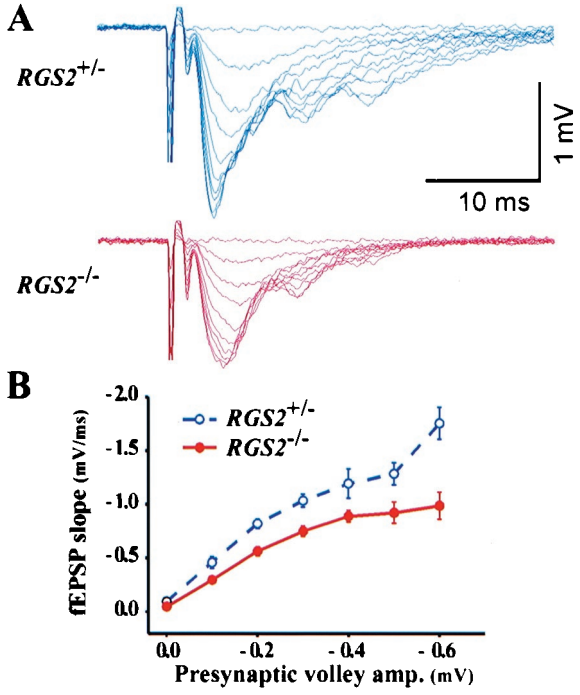

Fig. 7. Impaired basal electric activity in CA1 neurons of *rgs2*$^{-/-}$ mice. (*A* and *B*) Reduction of input/output relationship in CA1 pathway in *rgs2*$^{-/-}$ mice. Superimposed recordings of CA1 field excitatory postsynaptic potentials (fEPSP) evoked by electrical stimulation of Schaffer collateral input. Input: peak amplitude of presynaptic volley. Output: field EPSP slope measured at 10–65% rising phase of EPSP. Data are from seven hippocampus slices of four *rgs2*$^{+/-}$ and four *rgs2*$^{-/-}$ mice.

exploration test (3.5 ± 0.6 vs. 1.3 ± 0.6 pellets). In addition, *rgs2*$^{-/-}$ mice exhibited an increased response to acoustic startling. These data show that RGS2 controls neuronal circuits for aggression and anxiety.

RGS2 Role in Synapse Development and Basal Electrical Activity of Hippocampal CA1 Neurons. Fear and anxiety usually involve the amygdala, and certain components of fear can be affected by hippocampal inputs into the amygdala (26). Neurons from the CA1 region of the hippocampus project to the amygdala and removal of the hippocampus affects fear-based behavior (27). Moreover, it has also been proposed that RGS2 can regulate the activity of the G protein-coupled metabotropic glutamate re-

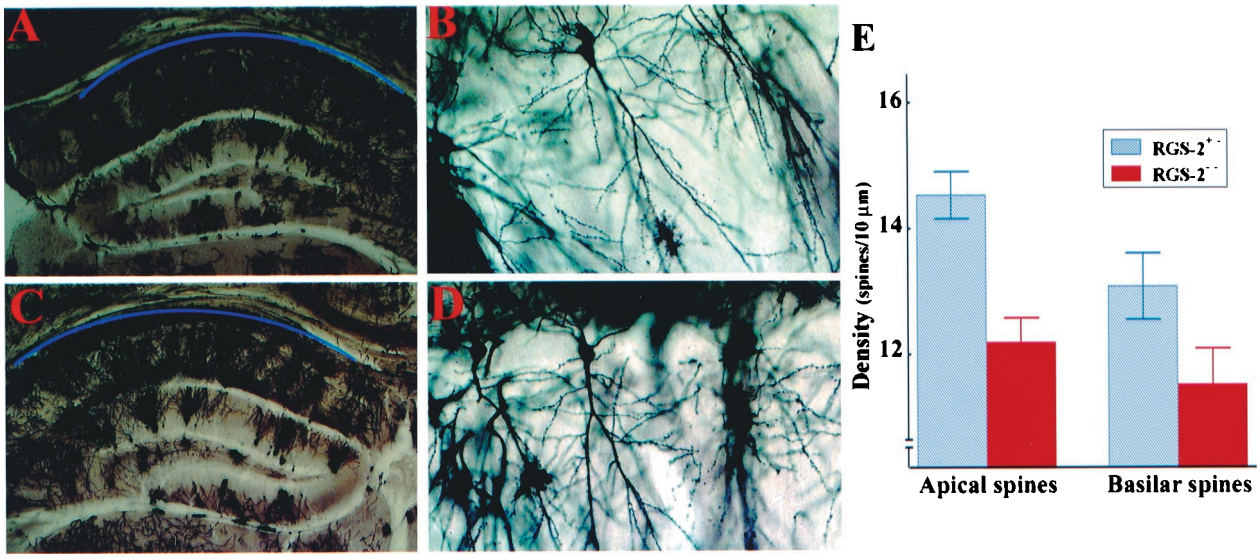

Fig. 6. Reduced spine density in CA1 hippocampal neurons of *rgs2*$^{-/-}$ mice. (*A–D*) Histology of hippocampus of *rgs2*$^{+/-}$ (*A* and *B*) and *rgs2*$^{-/-}$ (*C* and *D*) mice. Blue lines demarcate the CA1 neuron region. Normal structure of the CA1 region in *rgs2*$^{-/-}$ mice. Golgi–Cox staining, ×4 and ×200. (*E*) Reduced numbers of spines in *rgs2*$^{-/-}$ CA1 neurons. Densities (spines/10 µm ± SD) of apical and basilar spines were determined by camera lucida. Differences in apical and basilar spine densities were statistically significant (*t* test, $P < 0.005$).

ceptor 1, a receptor implicated in long-term synaptic plasticity in the hippocampus (28). Detailed examination of *rgs2*$^{-/-}$ mice revealed that the number of neurons in the hippocampus (Fig. 6 *A–D*), in other brain nuclei, the brainstem, cerebellum, and cortex (not shown) were not affected by RGS2 deficiency. Interestingly, whereas dendritic morphology and branching were comparable among cortical neurons of *rgs2*$^{+/-}$ and *rgs2*$^{-/-}$ mice, hippocampal CA1 neurons of *rgs2*$^{-/-}$ mice showed a significant decrease in the density of apical and basilar spines compared with those of *rgs2*$^{+/-}$ control littermates (Fig. 6*E*). The number of spines correlates with synapse numbers and neuronal plasticity (29). Importantly, the morphological deficit in spine numbers of *rgs2*$^{-/-}$ CA1 neurons correlated with significantly reduced electrical input/output relationship in these cells (Fig. 7 *A* and *B*). These data show that RGS2 has a role in synaptic development and basal electrical activity of hippocampal CA1 neurons.

Alterations in aggressive behavior and fear responses are important manifestations in highly prevalent psychiatric disorders such as depression or addictive behaviors. Because these disorders are responsible for a large social-economic burden, it is critical to identify gene products potentially involved in the initiation and/or progression of these behavioral "traits" into clinically manifest "disease." Multiple G protein-coupled receptors can regulate these behaviors, and pharmacological drugs that modulate these receptors have been developed to mitigate anxiety disorders and aggression. Our study provides genetic evidence that loss of a molecular regulators of G-protein signaling, RGS2, leads to impaired synaptic development in the hippocampus, reduced male aggressive behavior, and increased fear. Thus, RGS-family member such as RGS2 could be involved in the genetic predisposition to human neuropsychiatric disorders and could be potential targets for the generation of novel neuropharmacological drugs. *rgs2*$^{-/-}$ mice also provide a useful animal model to elucidate molecular mechanisms of fear and male aggression.

G protein-coupled receptors regulate fundamental processes of development, cell activation, and behavior. The present study shows that RGS2, a member of the RGS family, has important roles in T cell proliferation and IL-2 production. The T cell activation deficit observed *in vitro* translates into an impaired anti-virus response *in vivo*, indicating that RGS2 is physiologically relevant for normal T cell function and the establishment of an effective antiviral immune response. In addition, mice lacking RGS2 exhibit significantly reduced aggressive behavior and increased anxiety in the absence of any measured cognitive and motor deficits. Furthermore, morphological and electrophysiological analyses indicate that RGS2 expression is required for the generation of synaptic plasticity in hippocampal CA1 neurons. Thus, RGS2 is a critical regulator of T cell activation, neuronal function, and emotive fear, and aggression *in vivo*.

We are most grateful to K. Bachmaier, Y.-Y. Kong, and I. Kozieradzki for help and to M. Saunders for editing of the manuscript. J.M.P. and J.R. are supported by grants from the Medical Research Council of Canada. D.P.S. is supported by National Institutes of Health Grant AA11605.

1. Gilman, A. G. (1987) *Annu. Rev. Biochem.* **56,** 615–649.
2. Berman, D. M., Wilkie, T. M. & Gilman, A. G. (1996) *Cell* **86,** 445–452.
3. Watson, N., Linder, M. E., Druey, K. M., Kehrl, J. H. & Blumer, K. J. (1996) *Nature (London)* **383,** 172–175.
4. Hunt, T. W., Fields, T. A., Casey, P. J. & Peralta, E. G. (1996) *Nature (London)* **383,** 175–177.
5. Snow, B. E., Hall, R. A., Krumins, A. M., Brothers, G. M., Bouchard, D., Brothers, C. A., Chung, S., Mangion, J., Gilman, A. G., *et al.* (1998) *J. Biol. Chem.* **273,** 17749–17755.
6. Koelle, M. R. & Horvitz, H. R. (1996) *Cell* **84,** 115–125.
7. Berman, D. M. & Gilman, A. G. (1998) *J. Biol. Chem.* **273,** 1269–1272.
8. Chan, R. K. & Otte, C. A. (1982) *Mol. Cell. Biol.* **2,** 11–20.
9. Dohlman, H. G., Song, J., Ma, D., Courchesne, W. E. & Thorner, J. (1996) *Mol. Cell. Biol.* **16,** 5194–5209.
10. Siderovski, D. P., Strockbine, B. & Behe, C. I. (1999) *Crit. Rev. Biochem. Mol. Biol.* **34,** 215–251.
11. Chen, C. K., Burns, M. E., He, W., Wensel, T. G., Baylor, D. A. & Simon, M. I. (2000) *Nature (London)* **403,** 557–560.
12. Zeng, L, Fagotto, F., Zhang, T., Hsu, W., Vasicek, T. J., Perry 3rd, W. L., Lee, J. J., Gumbiner, B. M. & Costantini, F. (1997) *Cell* **90,** 181–192.
13. Siderovski, D. P., Heximer, S. P. & Forsdyke, D. R. (1994) *DNA Cell Biol.* **13,** 125–147.
14. Heximer, S. P., Cristillo, A. D. & Forsdyke, D. R. (1997) *DNA Cell Biol.* **16,** 589–598.
15. Ingi, T., Krumins, A. M., Chidiac, P., Brothers, G. M., Chung, S., Snow, B. E., Barnes, C. A., Lanahan, A. A., Siderovski, D. P., Ross, E. M., *et al.* (1998) *J. Neurosci.* **18,** 7178–7188.
16. Burchett, S. A., Volk, M. L., Bannon, M. J. & Granneman, J. G. (1998) *J. Neurochem.* **70,** 2216–2219.
17. Heximer, S. P., Watson, N., Linder, M. E., Blumer, K. J. & Hepler, J. R. (1997) *Proc. Natl. Acad. Sci. USA* **94,** 14389–14393.
18. Beadling, C., Druey, K., Richter, G., Kehrl, J. & Smith, K. A. (1999) *J. Immunol.* **162,** 2677–2682.
19. Tseng, C-C. & Zhang, X. Y. (1998) *Endocrinology* **139,** 4470–4475.
20. Liu, Q., Oliveira-Dos-Santos, A. J., Mariathasan, S., Bouchard, D., Jones, J., Sarao, R., Kozieradzki, I., Ohashi, P., Penninger, J. M. & Dumont, D. (1998) *J. Exp. Med.* **188,** 1333–1342.
21. Penninger, J. M., Fischer, K. D., Sasaki, T., Kozieradzki, I., Le, J., Tedford, K., Bachmaier, K., Ohashi, P. S. & Bachmann, M. F. (1999) *Eur. J. Immunol.* **29,** 1709–1718.
22. Whishaw, I. Q., Haun, F. & Kolb, B. (1999) in *Modern Techniques in Neuroscience*, eds. Windhorst, U. & Johansson, H. (Springer, New York).
23. Lu, Y. M., Roder, J. C., Davidow, J. & Salter, M. W. (1998) *Science* **279,** 1363–1367.
24. Kehrl, J. H. (1998) *Immunity* **8,** 1–10.
25. Parmigiani, S., Ferrari, P. F. & Palanza, P. (1998) *Neurosci. Biobehav. Rev.* **23,** 143–153.
26. Rogan, M. T. & LeDoux, J. E. (1996) *Cell* **85,** 469–475.
27. White, N. M. & McDonald, R. J. (1993) *Behav. Brain. Res.* **55,** 269–281.
28. Kammermeier, P. J. & Ikeda, S. R. (1999) *Neuron* **22,** 819–829.
29. Moser, M. B. (1999) *Cell. Mol. Life Sci.* **55,** 593–600.